

Li-Hong Bao<sup>1,2\*</sup>,  
Hai-Teng Ma<sup>1</sup>

# Preparation of Temperature-Sensitive Polyurethanes Based on Modified Castor Oil

DOI: 10.5604/01.3001.0010.1686

<sup>1</sup>School of Materials Science and Engineering,  
Beijing Institute of Fashion Technology,  
Beijing 100029, China  
\* E-mail: blh332@163.com

<sup>2</sup>Beijing Key Laboratory of Clothing  
Materials R&D and Assessment,  
Beijing 100029, China

## Abstract

A series of temperature-sensitive polyurethanes (TSPUs) with polytetrahydrofuran glycol (PTMG), poly(ethylene glycol) (PEG) and maleic anhydride modified castor oil (MCO) as soft segments were prepared in this paper. The morphology of the temperature-sensitive polyurethane films was characterised by SEM, DSC and WAXD. SEM studies were also carried out to investigate the surface structure of coated and uncoated fabrics. The water vapour permeability of the coated and uncoated fabrics were measured as well. The results showed that a nonporous TSPU layer was formed on the coated fabric surface. The tailor-made TSPUs had one to three soft segment crystal melting point temperatures, with the lower peak temperature  $T_{pm1}$  belonging to the soft segment PTMG and the higher peak temperature  $T_{pm2}$  to the hydrophilic soft segment PEG2000. The water vapour permeability of TSPUs coated fabrics increased with an increase in PEG2000 concentration and PEG molecular weight, but decreased with an increase in the hard segment content, and triggered around the soft segment crystal melting point temperature of TSPUs.

**Key words:** modified castor oil, temperature-sensitive polyurethane, waterproof fabrics, breathable fabrics.

## ■ Introduction

Researches on temperature-sensitive polyurethanes (TS-PU) have been of great interest due to their wide application in the textile industry [1-3], medicine [4-5], environmental fields [6-8], packaging [9-10] and so on. For example, combining ordinary fabrics with TSPU membranes can lead to the development of a type of smart textiles which would not only be waterproof at any temperature because of the dense polymer film, but also present variable water vapour permeability in response to the surrounding temperature [11].

In 1992, Horii et al. claimed to have prepared a polyurethane with  $T_g$  at 0-60 °C, which can be used on fabrics, with the evaporation of body sweat to the outside world controlled by adjusting the  $T_g$  area of the polyurethane; this may be the first report on TS-PU used to develop smart textiles [12]. In 2006, X.M. Ding et al. reported that the crystalline properties of PUs, including the degree of crystallinity and crystal melting temperature, depend on the chemical structure of the polyol and hard segment concentration. With the temperature range of crystal melting from 10 °C to 40 °C, the water vapour permeability of the PU membranes increased significantly with increasing temperature [13]. In 2010, Shi Huanhuan et al compared the properties of two types of thermosensitive polyurethane (TSPU) and a polyurethane elastomer (EPU). They found that the TSPU showed a separate phase behavior and a phase transi-

tion temperature in the normal wearing temperature range, and the free volume holes of TSPU showed dramatic changes when the temperature exceeded the phase transition temperature. While for EPU no phase transition could be observed. Leathers finished with TSPU had lower water vapour permeability (WVP) at low temperature and higher WVP at high temperature [14]. Some other researches have also been carried out regarding the preparation, properties and water vapour permeability of TSPUs and their coated fabrics [15-18]. Furthermore we seldom see such PUs made from natural materials.

Castor oil is a natural triglyceride of ricinoleic acid. It has an effective hydroxyl functionality of 2.7. Once polymerised, the long pendant chains of the fatty acids impart flexibility and hydrolysis resistance to the polymer. Urethane polymers prepared from castor oil exhibit excellent abrasion resistance [19]. Therefore the object of the present study was to synthesise a series of TSPUs used as fabric coatings with modified natural castor oil, and then investigate the relationship between the composition and properties of TSPUs. For this purpose, in the work reported here, three series of TSPUs were synthesised by means of molecular design, and then their microstructures were investigated using differential scanning calorimetry (DSC), wide-angle X-ray (WAXD) and a scanning electron microscope (SEM). The water vapour permeability of the TSPU membrane was measured according to GB/T 12704.1-2009.

## ■ Experimental

### Materials

Polytetrahydrofuran glycol (PTMG; Aladdin) with  $M_n = 2000 \text{ g mol}^{-1}$  and Poly(ethylene glycol) (PEG,  $M_n = 400, 600, 800, 1000, 2000$ , respectively) were dried and degassed for 5 h at 80 °C, 1~2 mmHg, before use. 4,4'-methylenediphenyl diisocyanate (MDI; Aladdin) was used to synthesise TSPU samples without further treatment, and Dimethylformamide (DMF; Fuchen Chemical Reagents Factory, Tianjin, China), 1,4-butanediol (BDO; Fuchen Chemical Reagents Factory, Tianjin, China) and maleic anhydride modified castor oil (MCO prepared as in our previous work) [20] were dried with molecular sieves for several days before use.

In this study, three series of thermoplastic polyurethanes with the crystal melting transition as the switching temperature were synthesised. The formula of the preparation of TSPU samples is shown in **Table 1**.

### Synthesis of TSPU

The reaction was carried out in a 250 ml conical flask equipped with a mechanical stirrer. PTMG and PEG were mixed at 35 °C, MCO and MDI dissolved in DMF were placed in a reactor, and the mixture kept at 35 °C until the theoretical NCO value, as determined by the di-n-butylamine titration method, was reached. After that, BDO was added to the mixture as a chain extender and the reaction pro-

ceeded at 85 °C until no NCO groups were detected. The reaction was kept in a nitrogen gas atmosphere to avoid the influence of moisture during the synthesis process.

### TSPU film preparation

The PU solution was cast onto a Teflon pan and kept at 65 °C for 24 h. Then the DMF was removed under a vacuum at 80 °C for 10 h. The thickness of the films were about 1 mm.

### Coating of fabrics

Scoured and bleached white polyester fabrics of 120 g/m<sup>2</sup> weight (Jian Ai Textile Co., Ltd. Shaoxing city, China) were coated by a knife over a roller machine (Werner Mathis AG, Switzerland). The thickness of the coating was controlled at 0.10 mm. The coated fabrics were dried at 90 °C for 20 min in order to remove the DMF and then cured at 140 °C for 3 min.

### Equipments and measurements

The surface and cross section of TSPU film and the surface of the coated and uncoated fabrics were observed by a Scanning Electron Microscope (SEM) (JSM-6360IV JEOL LTD., Japan).

Differential scanning calorimetry data for TSPUs were obtained by DSC 6200 (Seiko Instruments Inc. Japan). Each sample was scanned from -50 °C to 120 °C at a scanning rate of 10 °C/min under a dry nitrogen purge. All runs were carried out with a sample weight of 5-10 mg.

Wide-angle X-ray diffraction (WAXD) patterns of the TSPU films were recorded on a D/max-1200 X-ray diffractometer with Cu K $\alpha$  radiation ( $\lambda = 1.5405 \times 10^{-10}$  m), and the samples were examined with 20 ranging from 5° to 50° at a scanning rate of 5°/min.

The mass transfer of the coated and uncoated fabrics was measured from the water vapor permeability (WVP), measured according to GB/T 12704.1-2009. Round mouth conical plastic cups with a diameter of 60 mm and height of 19 mm were filled with anhydrous calcium chloride. The uncoated and coated fabrics were placed over the top of the cups, ensuring perfect sealing between the cup and fabric sample. The gap between the fabric and desiccant surface was about 4 mm. Cups were placed in a constant

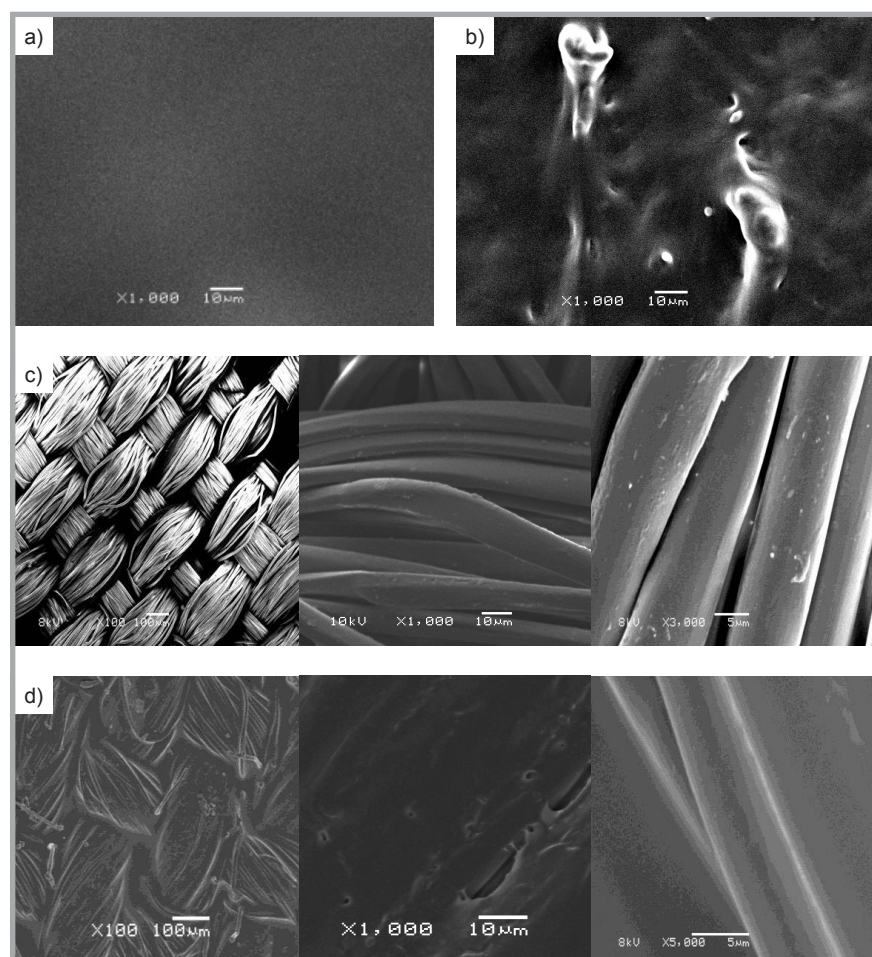


**Figure 1.** SEM image of: a) surface section of TSPU-3-4 film, b) cross section of TSPU-3-4 film, c) uncoated fabric, d) coated fabric with TSPU-3-4.

temperature chamber at the desired temperature (10, 16, 20, 26, 32, 38, 44, 54 °C). During all WVP measurements, air surrounding the fabric had a constant temperature and 90% relative humidity. An average of 3 different samples was used for each WVP measurement, calculat-

ed using the following formula and expressed in units of g m<sup>-2</sup>d<sup>-1</sup>, where d is a day (24 h).

$$WVP = \frac{G}{A \cdot t}$$

Where G = weight change in gm, t = duration test in hours, and A = test area in m<sup>2</sup>.

**Table 1.** Data relating to polyurethanes prepared. Note: "Hard segment content. Calculated form  $(M_{MDI} + M_{BDO}) / (M_{MDI} + M_{BDO} + M_{PTMG} + M_{PEG} + M_{MCO}) \times 100\%$ ".

Sample No	Feed molar ratio			HSS <sup>a</sup> , %	PEG content, %	PEG composition
	PTMG/MCO/PEG	MDI	BDO			
TSPU-1-1	0.48/0.40/0.12	2.3	1.3	30.1	10.4	PEG2000
TSPU-1-2	0.43/0.40/0.17	2.3	1.3	30.1	14.7	PEG2000
TSPU-1-3	0.36/0.41/0.23	2.3	1.3	30.2	19.9	PEG2000
TSPU-1-4	0.32/0.40/0.28	2.3	1.3	30.1	24.3	PEG2000
TSPU-1-5	0.26/0.40/0.34	2.3	1.3	30.1	29.5	PEG2000
TSPU-2-1	0.40/0.40/0.16	1.5	0.5	21.2	15.0	PEG2000
TSPU-2-2	0.40/0.40/0.16	1.8	0.8	24.9	15.0	PEG2000
TSPU-2-3	0.42/0.41/0.16	2.0	1.0	27.0	15.0	PEG2000
TSPU-2-4	0.40/0.40/0.17	2.3	1.3	30.4	15.0	PEG2000
TSPU-2-5	0.37/0.40/0.18	2.6	1.6	34.4	15.0	PEG2000
TSPU-3-1	0.10/0.40/0.50	2.0	1.0	44.2	15.0	PEG400
TSPU-3-2	0.16/0.44/0.40	2.0	1.0	36.8	15.0	PEG600
TSPU-3-3	0.33/0.32/0.35	2.0	1.0	30.9	15.0	PEG800
TSPU-3-4	0.40/0.30/0.30	2.0	1.0	29.5	15.0	PEG1000

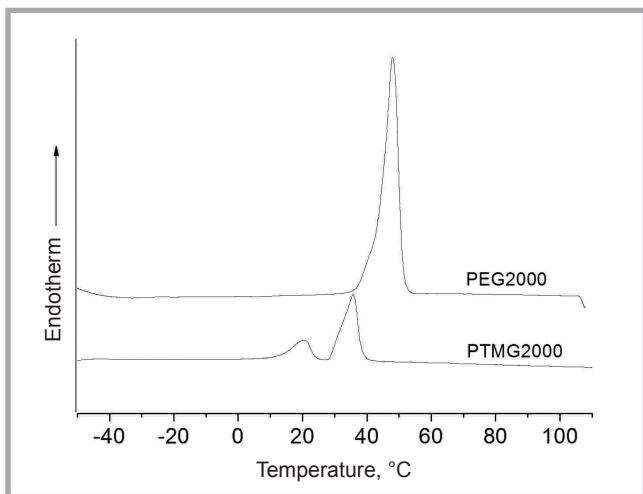


**Figure 2.** DSC curves of PEG2000 and PTMG2000.

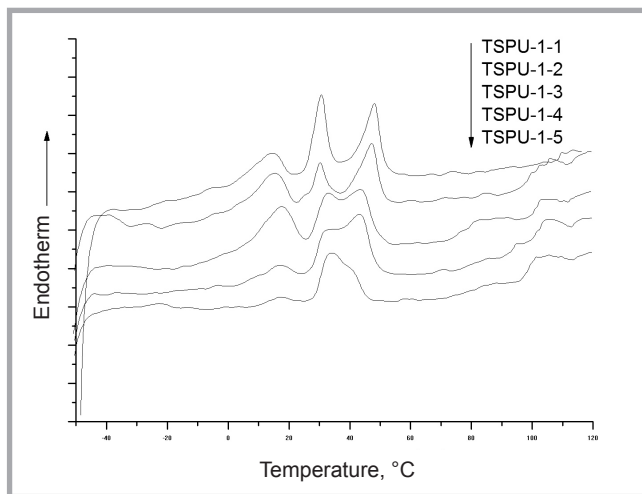


**Figure 3.** DSC curves of TSPUs with varied PEG2000 contents.

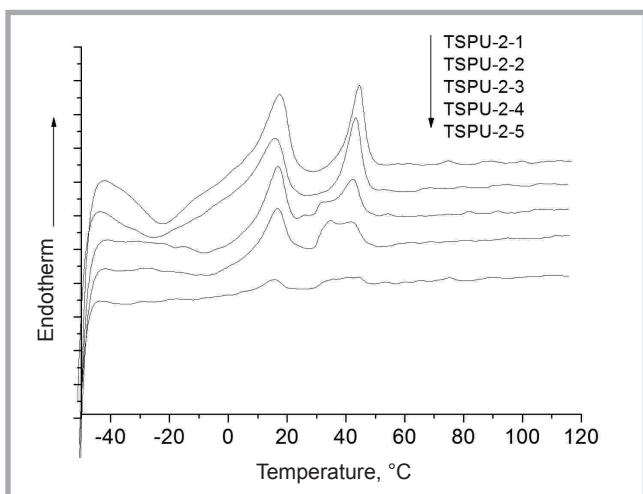


**Figure 4.** DSC curves of TSPUs with different hard segment contents.

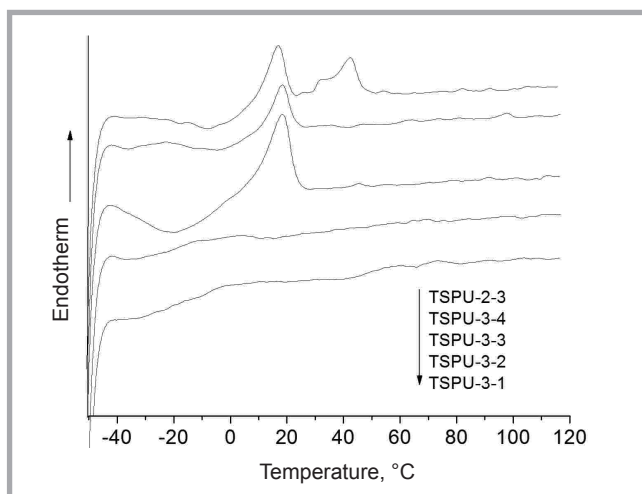


**Figure 5.** DSC curves of TSPUs with different PEG as hydrophilic soft segment.

## Results and discussion

### SEM micrograph

SEM pictures of the surface section and cross section of the TSPU film are shown in **Figures 1.a** and **1.b**. We could observe that the polymer film has a smooth surface, no clear contrast and a channel through the film. Hence we can conclude that the TSPU film was dense and with no pores in it.

Observation of the uncoated polyester fabrics **Figure 1.c** by SEM revealed that the surfaces are porous. In contrast, most of the fiber apertures are filled up by polymer after coating **Figure 1.d**. The nonporous TSPU layer was formed continuously over the surface of the coated fabric. The presence of the nonporous TSPU layer suggested that the water vapour permeability of the coated fabrics originates from the properties of TSPU

itself. Therefore the chemical structure of TSPU plays a major role in the breathability of coated fabrics.

### Differential scanning calorimetry

**Figures 2-5** shows the DSC curves of pure polyol and the resulting TSPUs, and **Table 2** lists the peak temperatures ( $T_{pm}$ ) and heat of fusion ( $\Delta H_f$ ) of the crystalline peaks. From **Figure 2**, it is observed that pure polyols PEG2000 and PTMG2000 were crystalline with sharp endothermic peaks. **Figure 3** to **Figure 5** show that there were one to three peaks in these series of TSPUs, with the lower peak temperature  $T_{pm1}$  at 14.24~17.57 °C belonging to the soft segment PTMG 2000 and the higher peak temperature  $T_{pm2}$  at 40.99~48.11 °C belonging to the hydrophilic soft segment PEG2000. That is, in a mixed soft segment block TSPU, each soft block forms a crystalline structure separately. Therefore separate endothermic peaks were appeared for subsequent blocks [21]. It can be observed that  $T_{pm1}$  and  $T_{pm2}$  were both lower than for the pure polyols. From **Figure 3** we can see that with an increase in PEG2000 content, with  $T_{pm1}$  increasing,  $T_{pm2}$  decreasing, the crystalline peaks for PTMG2000 decreasing, and the total  $\Delta H_f$  decreasing, which implies that the crystallinity of TSPU decreases, as proved by WAXD, which may be due to the hindrance of more polyether groups in PEG2000.

DSC curves of the TSPUs with different hard segment contents are shown in **Figure 4**. It is observed that an increase in the hard segment content led to a decrease in  $\Delta H_f$  of the TSPUs. As we know, the hard segments act as a reinforcing filler in soft matrices and hinder the crystallisation process of the soft domains [21-22]. **Figure 5** indicates that as the  $M_n$  of the hydrophilic segment PEG increased from 800 to

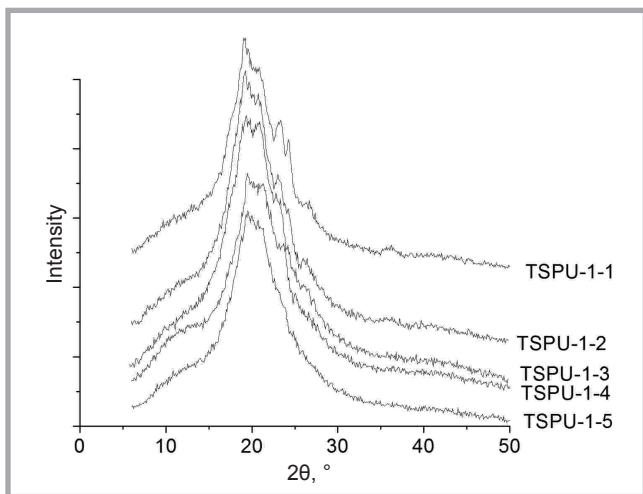


**Figure 6.** WAXD curves of TSPUs with varied PEG2000 contents.

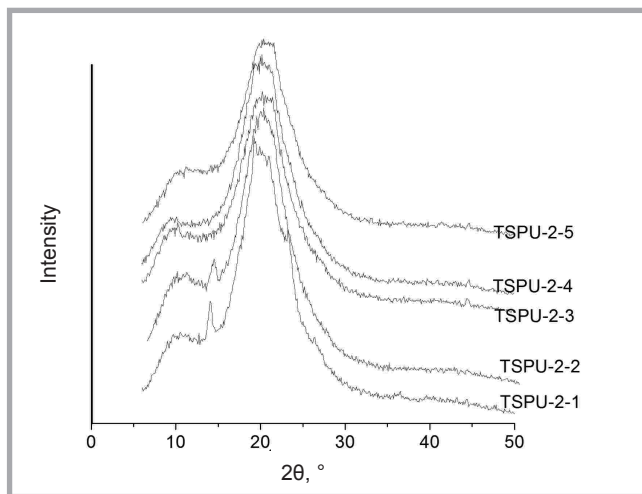


**Figure 7.** WAXD curves of TSPUs with different hard segment contents.

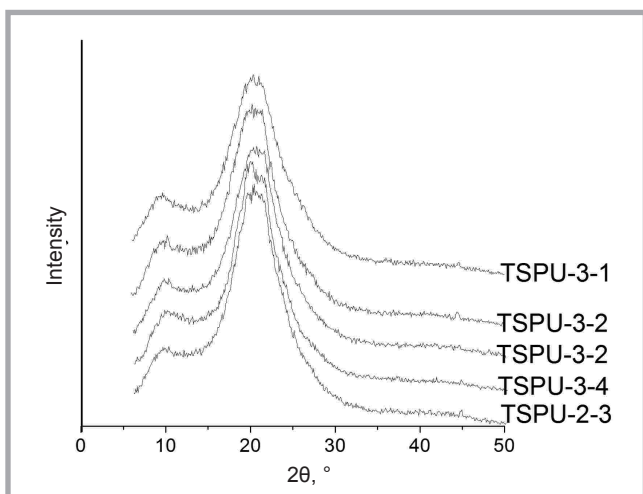


**Figure 8.** WAXD curves of TSPUs with different PEG as hydrophilic soft segment.

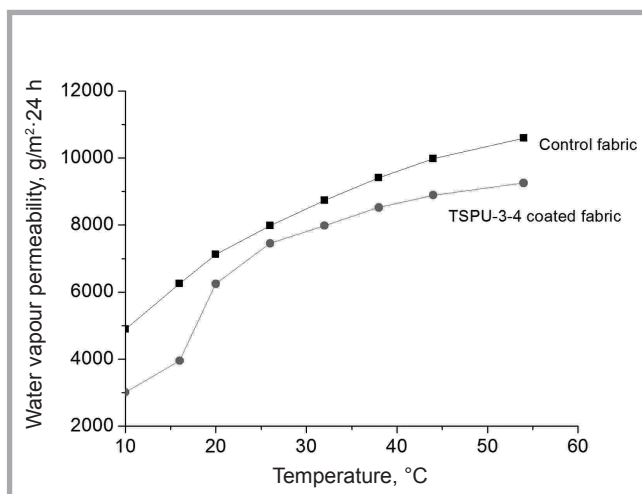


**Figure 9.** Water vapour permeability of control fabric and TSPU-3-4 coated fabric.

2000, it enhanced the shifting of the primary endothermic peak due to the ordering of the crystalline PEG domain. When the  $M_n$  of PEG was lower than 2000, no crystalline peak was seen for PEG. When the  $M_n$  of PEG was lower than 800, the PU behaved rather as amorphous material almost without any crystalline melting peak. These results are supported by the measurements of WAXD.

### Results from WAXD

**Figures 6–8** show typical X-ray diffraction profiles obtained for the TSPUs. Most of the diffraction profiles showed an amorphous, diffused diffraction. It is likely that some soft segment-hard segment phase mixing in the system disturbed the soft segment crystallisation, which may account for the broader diffraction. As the WAXD were performed at a temperature quite near or above the crystal melting temperature of TSPUs, the X-ray diffrac-

**Table 2.** Thermal properties of TSPUs.

No	$T_{pm1}$ , °C	$T_{pm2}$ , °C	$\Delta H_f$ , mJ/mg
PTMG2000	20.3	35.7	58.7
PEG2000	–	54.1	179
TSPU-1-1	14.24	48.11	41.3
TSPU-1-2	15.66	47.41	32.7
TSPU-1-3	17.11	44.50	30.5
TSPU-1-4	17.25	43.92	24.8
TSPU-1-5	17.57	41.39	20.1
TSPU-2-1	17.53	44.43	45.5
TSPU-2-2	17.28	44.48	42.6
TSPU-2-3	17.54	43.04	36.2
TSPU-2-4	17.05	42.56	32.4
TSPU-2-5	16.17	40.99	28.9
TSPU-3-1	–	–	–
TSPU-3-2	–	–	–
TSPU-3-3	18.53	–	18.0
TSPU-3-4	18.38	–	30.6

**Table 3.** Water vapour permeability results of coated and uncoated fabrics.

No	WVP, g/(m <sup>2</sup> ·d)
Control fiber	9475
TSPU-1-1	7932
TSPU-1-2	8224
TSPU-1-3	8400
TSPU-1-4	8751
TSPU-1-5	9097
TSPU-2-1	9240
TSPU-2-2	9154
TSPU-2-3	9036
TSPU-2-4	8846
TSPU-2-5	8630
TSPU-3-1	7910
TSPU-3-2	8482
TSPU-3-3	8460
TSPU-3-4	8527

tions could not detect all characteristic diffractions arising from the crystallites of PTMG and PEG. A small number of weak, sharp peaks observed is the proportion of residual crystallites [23]. In **Figure 6** all diffraction profiles showed small peaks at  $2\theta = 19.2^\circ$  and  $23.2^\circ$ , except TSPU-1-5, which became smaller with an increase in PEG2000 concentration. In **Figure 7**, TSPU-2-1 with the least hard segment content shows small diffraction peaks, and with an increase in the hard segment content the diffraction became broader and smoother, with the aggregation of hard segments in the TSPU system significantly disturbing the ordered packing of soft segments, which leads to imperfect crystallisation of the segments [24]. In **Figure 8**, no small diffraction peaks are seen. The absence of crystalline diffraction in samples analysed at ambient temperature is the consequence of the melting of the crystallines at the analysis temperature. Notwithstanding the temperature effect, the WAXD pattern is generally in line with the DSC profiles.

### Water vapour permeability

Water vapor permeability results of the coated and uncoated fabrics at  $38^\circ\text{C}$  are shown in **Table 3**. SEM pictures show that the polymeric films on the coated fabric are nonporous, therefore the TSPU film's properties will play a major role in the permeability of water vapour. In these cases, water vapour transmission would occur through the nonporous membrane in three stages i.e., sorption-diffusion-desorption. The water vapour permeability study results show that with an increase in hydrophilic PEG2000 content, the WVP increases, and as the TSPU hard-segment content increases, WVP tends to slightly

decrease. When PEG contents were kept at 15%, the WVP increases with an increase in PEG molecular weight.

Take TSPU-3-4 as an example, where the thermo-sensitive properties of TSPU was studied. **Figure 9** shows the relationships between the water vapour permeability of the control fabric and TSPU-3-4 coated fabric with temperature. When the temperature rises from  $10^\circ\text{C}$  to  $54^\circ\text{C}$ , WVP increased significantly. The increase in temperature will increase the difference in saturation vapour pressure between the cup and surroundings, which will enhance permeability through the coated and uncoated fabrics. The water vapour permeability of TSPU-3-4 coated fabrics increased abruptly at the soft segment crystal melting point, due to the increasing mobility of the soft segment (polyol) phase, which is enhanced at the melting temperature of the soft domain. The micro-Brownian motion of the soft segment at the crystal melting point temperature would increase the inter-molecular gap large enough to allow more water vapour molecules to pass through the polymer films [25]. While the WVP of the control fabric increased gradually with an increase in temperature.

### Conclusions

Crystal melting properties and water vapor permeability were presented for a series of temperature sensitive polyurethanes based on PTMG, MCO as soft segments and PEG as a hydrophilic group. The crystallinity of TSPU decreases with an increase in PEG2000 content. An increase in hard segment content led to a decrease in  $\Delta H_f$  of the TSPUs. When the  $M_n$  of PEG was lower than 2000, no crystalline peak was detected for PEG. XRD analysis showed TSPUs to possess both defined and diffused crystallinity at ambient temperatures. Crystallinity decreased with an increase in PEG2000 concentration and hard segment content. SEM studies showed that the TSPU film has a smooth surface, with no pores in it, and that the coated fabric surface was covered by a nonporous TSPU layer. The water vapour permeability of TSPU coated fabrics was influenced by the primary chemical structure of TSPU. The water vapour permeability of TSPU coated fabric increased significantly around the soft segment crystal melting point temperature, when the chain mobility of the soft segment was enhanced by the phase transition. The temperature sensitive wa-

ter vapour permeability of the tailor-made TSPUs coated fabrics would be applicable in developing smart clothing.

### Acknowledgements

This research was supported by the National Natural Science Foundation of China (No.21304004).

### References

1. Lv Haining, Xue Yuan, Cai Zaisheng, et al. Microporous membrane with temperature-sensitive breathability based on PU/PNIPAAm semi-IPN. *Journal of Applied Polymer Science* 2012;124:E2-E8.
2. Hu Zhou, Yi Chen, Haojun Fan, et al. Water vapor permeability of the polyurethane/TiO<sub>2</sub> nanohybrid membrane with temperature sensitivity. *Journal of Applied Polymer Science* 2008;109: 3002-3007.
3. Bin Zhai, Chi Zhang, Fuqiang Zhang, et al. Covalent modification of temperature-sensitive breathable polyurethane with carbon nanotubes. *Journal Soft Materials* 2016; 14: 272-277.
4. Baohua Liu, Jinlian Hu, Qinghao Meng. Nonwoven supported temperature-sensitive poly(N-isopropylacrylamide)/polyurethane copolymer hydrogel with antibacterial activity. *Journal of Bio-medical Materials Research Part B: Applied Biomaterials* 2009; 89B: 1-8.
5. Franklin M.-M, Emilio Bucio, Beatriz M, et al. Temperature- and pH-sensitive IPNs grafted onto polyurethane by gamma radiation for antimicrobial drug-eluting insertable devices. *Journal of Applied Polymer Science* 2014; 131: 39992.
6. Karakas H, Sarac AS, Polat T, et al. Polyurthane nanofibers obtained by electrospinning process. *International Journal of Biological, Biomolecular, Agricultural, Food and Biotechnological Engineering* 2013; 7(3): 177-180.
7. Zhou Hu, Yu Bin, Zhou Jie, et al. Synthesis and characterization of thermal- and pH-Sensitive polyurethane hydrogels with different transition temperature. *Nanoscience and Nanotechnology Letters* 2016; 8: 647-653.
8. Mason B P, Whittaker M, Hemmer J, et al. A temperature-mapping molecular sensor for polyurethane-based elastomers. *Appl. Phys. Lett.* 2016; 108: 041906.
9. Hu Zhou, Bin Yu, Ruiping Xun, et al. Novel temperature-sensitive and pH-sensitive polyurethane membranes: preparation and characterization. *Asia-Pacific Journal of Chemical Engineering* 2015; 10: 193-200.
10. Hu Zhou, Huanhuan Shi, Haojun Fan and Jixin Yuan. Thermo-sensitive polyurethane membrane with controllable water vapor permeation for food packaging. *Macromolecular Research* 2009; 17: 528-532.
11. Duan Ya-feng, Quan Heng, Hu Ling-ling. Study of polyurethane used for tempera-

- ture-sensitive waterproof and breathable fabric. *Silk Monthly* 2007; 12: 34-36.
12. Horii F, Maruyama H, Hayashi S, et al. Moisture-permeable water-proof fabric and its production. *JPH04370276 (A)* 1992; 12, 22.
  13. Ding X M, Hu J L, Tao X M, et al. Preparation of temperature-sensitive polyurethanes for smart textiles. *Textile Research Journal* 2006; 76: 406-413.
  14. Huanhuan Shi, Yi Chen, Haojun Fan, et al. Thermosensitive polyurethane film and finished leather with controllable water vapor permeability. *Journal of Applied Polymer Science* 2010; 117: 1820-1827.
  15. QUAN Heng, WU Dan and HAN Jing. Study on the structure of polyether polyurethane and its waterproofing & breathable properties. *TEXTILE AUXILIARIES* 2012; 29: 8-11.
  16. Ding XM, Hu JL. Morphology and water vapor permeability of temperature-sensitive polyurethanes. *Journal of Applied Polymer Science* 2008; 107: 4061-4069.
  17. Han H R. Shape memory and breathable waterproof properties of polyurethane nanowebs. *Textile Research Journal* 2013; 83: 76-82.
  18. Mondal S and Hu J L. Free volume and water vapor permeability of dense segmented polyurethane membrane. *Journal of Membrane Science* 2006; 280: 427-432.
  19. Anupama Kaushik Paramjit Singh. Kinetic Study of polyurethane reaction between castor Oil/TMP polyol and diphenyl methane diisocyanate in bulk. *International Journal of Polymeric Materials and Polymeric Biomaterials* 2006; 55:549-561.
  20. Bao Li-Hong, Lan Yun-Jun and Zhang Shu-Fe. Synthesis and properties of waterborne polyurethane dispersions with ions in the soft segments. *Journal of Polymer Research* 2006; 13: 507-514.
  21. Mondal S and Hu J L. Water vapor permeability of cotton fabrics coated with shape memory polyurethane. *Carbohydrate Polymer* 2007; 67: 282-287.
  22. Qi Cao, Shaojun Chen and Jinlian Hu, et al. Study on the Liquefied-MDI-Based shape memory polyurethanes. *Journal of Applied Polymer Science* 2007; 106: 993-1000.
  23. Dyana Merline J, Reghunadhan C P, Gouri Nair C, et al. Polyether polyurethanes: Synthesis, characterization, and thermoresponsive shape memory properties. *Journal of Applied Polymer Science* 2008; 107: 4082-4092.
  24. Shaojun Chen, Qi Cao, Bo Jing, et al. Effect of Microphase-separation promoters on the shape-memory behavior of polyurethane. *Journal of Applied Polymer Science* 2006; 102: 5224-5231.
  25. Ding X M, Hu JL and Tao XM. Effect of crystal melting on water vapor permeability of shape-memory polyurethane film. *Textile Research Journal* 2004; 74: 39-43.

**The Scientific Department of Unconventional Technologies and Textiles** specialises in interdisciplinary research on innovative techniques, functional textiles and textile composites including nanotechnologies and surface modification.

Research are performed on modern apparatus, *inter alia*:

- Scanning electron microscope VEGA 3 LMU, Tescan with EDS INCA X-ray microanalyser, Oxford
- Raman InVia Reflex spectrometer, Renishaw
- Vertex 70 FTIR spectrometer with Hyperion 2000 microscope, Brüker
- Differential scanning calorimeter DSC 204 F1 Phenix, Netzsch
- Thermogravimetric analyser TG 209 F1 Libra, Netzsch with FT-IR gas cuvette
- Sigma 701 tensiometer, KSV
- Automatic drop shape analyser DSA 100, Krüss
- PGX goniometer, Fibro Systems
- Particle size analyser Zetasizer Nano ZS, Malvern
- Labcoater LTE-S, Werner Mathis
- Corona discharge activator, Metalchem
- Ultrasonic homogenizer UP 200 st, Hielscher

The equipment was purchased under key project - POIG.01.03.01-00-004/08 Functional nano- and micro textile materials - NANOMITEX, co-financed by the European Union under the European Regional Development Fund and the National Centre for Research and Development, and Project WND-RPLD 03.01.00-001/09 co-financed by the European Union under the European Regional Development Fund and the Ministry of Culture and National Heritage.



*Textile Research Institute  
Scientific Department of Unconventional Technologies and Textiles  
Tel. (+48 42) 25 34 405  
e-mail: cieslakm@iw.lodz.pl*